

# An advanced tool integrating failure and sensitivity analysis to novel modeling for stormwater flooding volume

Francesco Fatone<sup>1</sup>, Bartosz Szeląg<sup>2</sup>, Przemysław Kowal<sup>3</sup>, Arthur McGarity<sup>4</sup>, Adam Kiczko<sup>5</sup>, Grzegorz Wałek<sup>6</sup>, Ewa Wojciechowska<sup>3</sup>, Michał Stachura<sup>7</sup>, Nicolas Caradot<sup>8</sup>

<sup>1</sup> Department of Science and Engineering of Materials, Environment and Urban Planning-SIMAU, Polytechnic University of Marche Ancona, 60121 Ancona, Italy

<sup>2</sup> Faculty of Environmental, Geomatic and Energy Engineering, Kielce University of Technology, 25-314 Kielce, Poland

<sup>3</sup> Faculty of Civil and Environmental Engineering, Gdansk University of Technology, 80-233, Gdansk, Poland

<sup>4</sup> Department of Engineering, Swarthmore College, 500 College Ave., Swarthmore, PA, 19081, United States

<sup>5</sup> Institute of Environmental Engineering, Warsaw University of Life Sciences-SGGW, 02-797 Warsaw, Poland

<sup>6</sup> Institute of Geography and Environmental Sciences, Jan Kochanowski University in Kielce, 25 – 406, Kielce, Poland

<sup>7</sup> Faculty of Law and Social Sciences, Jan Kochanowski University, 25 – 406, Kielce, Poland

<sup>8</sup> Berlin Competence for Water, Cicerostr. 24, 10709 Berlin, Germany

Correspondence to: Bartosz Szeląg (bszelag@tu.kielce.pl)

## Section 1. Uncertainty analysis - GLUE

The problem of parameter identification in the GLUE method is formulated in the form of the Bayesian estimation relation (Beven and Binley, 1992):

$$P(Q/\theta) = \frac{L(Q/\theta)P(\theta)}{\int L(Q/\theta)P(\theta)} \quad (1)$$

where  $P(\theta)$  stands for *a priori* (Tab. S1) parameter distribution; the *a priori distribution* of SWMM parameters represents the initial assumption of parameter variability. In the case of mathematical models used to describe surface runoff, usually there is no knowledge of the structure of its distribution and the range of acceptable parameter values resulting from their physical interpretation is known at most. In the analysed case it was assumed that the distribution has uniform character (. In the present discussion the following form of the likelihood function was used (Romanowicz and Beven, 2000):

$$L(Q/\theta) = \exp\left(\frac{r_t}{\varepsilon \cdot V(r_t)}\right) \quad (2)$$

$V(\cdot)$  – variance,  $r_t$  - mean of the sum of squares of deviations of simulated value from measured value calculated as  $r_t = \frac{1}{l} \cdot \sum_{z=1}^l (Q_o - \hat{Q}_l)^2$  (where:  $Q_o$  and  $\hat{Q}_l$  denote  $z$ -th value from the times series of observed and computed flows;  $\varepsilon$  is a scaling factor for the variance of model residua, used to adjust the width of the confidence intervals. In Kiczko et al. (2018) study, the value of  $\varepsilon$  was determined, ensuring that 95% of observed discharge points is enclosed by 95% confidence intervals of the model output. Equation (1) is solved using the Monte Carlo method. In the first step, a sample of parameters is developed from an assumed *a priori* distribution. The model (SWMM in this case) is run with each combination of SWMM model

35 parameters (Tab. S1) and from the calculated and measured outflow hydrographs the values of the likelihood function and *a*  
 36 *posteriori* distributions are determined.

37

38 **Table S1. Ranges of SWMM model parameters**

39

Parameters	Unit	Range	
		Min	Max
Coefficient for flow path width ( $\alpha$ )	-	2.7	4.7
Retention depth of impervious areas ( $d_{imp}$ )	mm	0.8	4.8
Retention depth of pervious areas ( $d_{per}$ )	mm	0.8	6.8
Manning roughness coefficient for impervious areas ( $n_{imp}$ )	$m^{-1/3}\cdot s$	0.01	0.022
Manning roughness coefficient for pervious areas ( $n_{per}$ )	$m^{-1/3}\cdot s$	0.16	0.2
Manning roughness coefficient for sewer channels ( $n_{sew}$ )	$m^{-1/3}\cdot s$	0.01	0.048
Correction coefficient for sub-catchments slope ( $\gamma$ )	-	0.7	1.275
Correction coefficient for percentage of impervious areas ( $\beta$ )	-	0.8	1.375

40

41 **Table S2. Corrective variants for stormwater system**

42

Variants	Condition
I	$0.9 \cdot Imp$
II	$0.9 \cdot Imp + (d_{imp} = 3.5mm \ n_{imp} = 0.035 \ m^{-1/3}\cdot s)$
III	$0.9 \cdot Imp + (d_{imp} = 3.5mm \ n_{imp} = 0.035 \ m^{-1/3}\cdot s) + (n_{sew} = 0.012 \ m^{-1/3}\cdot s)$

43

## 44 Section 2. Measures of fit between computed results and measurements in a logistic regression model

45 At the computation stage, the goal was to find such a value of threshold cut off which would provide maximum fit of  
 46 simulation to measurement data. Thus, the subsequent cut-off values  $p_m$  were tested until the best fit of measurement data and  
 47 computation results was obtained (SENS, SPEC  $\rightarrow$  max of value). The fit of the calculation results to measurements was  
 48 evaluated with the following measures: sensitivity (SENS – determines correctness of classification in a set when the threshold  
 49 values are exceeded), specificity (SPEC – determines correctness of classification in a set when the threshold values are not  
 50 exceeded) and accuracy (Acc), which were discussed in detail in Harrell (2001).

51 - accuracy (Acc)

$$52 \quad Acc = \frac{TP+TN}{TP+TN+FP+FN} \quad (3)$$

53 - sensitivity (SENS)

$$54 \quad Sens = \frac{TP}{TP+FN} \quad (4)$$

55 and specificity (SPEC)

56

$$Spec = \frac{TN}{TN+} \quad (5)$$

57 where  $TP, TN, FP$ , and  $FN$  denote true positives (correctly identified of the  $\kappa \geq 13 \text{ m}^3 \cdot \text{ha}^{-1}$ ), true negatives  
 58 (correctly identified lack of  $\kappa \geq 13 \text{ m}^3 \cdot \text{ha}^{-1}$ ), false positives ( $\kappa < 13 \text{ m}^3 \cdot \text{ha}^{-1}$  incorrectly identified as  $\kappa \geq 13 \text{ m}^3 \cdot \text{ha}^{-1}$ )  
 59 and false negatives ( $\kappa \geq 13 \text{ m}^3 \cdot \text{ha}^{-1}$  incorrectly identified as  $\kappa < 13 \text{ m}^3 \cdot \text{ha}^{-1}$ ), respectively.

60

### 61 Section 3. Regional model of convective rainfall

62 To calculate the convective rainfall, the regional rainfall model for Poland was used (Kupczyk and  
 63 Suligowski, 2000; Suligowski, 2004). In this model the rainfall depth for the assumed rainfall duration is  
 64 determined from the formula:

$$65 \quad P_{con}(t_r) = a_1 \cdot t_r^2 + a_2 \cdot t_r + a_0 \quad (6)$$

66 where:  $t_r$  – duration of rainfall (min);  $P_{con}(t_r)$  – maximum convective rainfall depth (mm);  $a_0, a_1, a_2$  – empirical  
 67 coefficients determined by the method of least squares. The model includes data for 30 rainfall stations in Poland,  
 68 for which  $a_i$  ( $a_0, a_1, a_2$ ) coefficients were determined using rainfall data from the period of 20 - 30 years (Suligowski  
 69 2004). For the catchment area covered by the calculations (świętokrzyskie voivodship) the values are as follows:  
 70  $a_0 = 6.55$ ;  $a_1 = -1.10$ ,  $a_2 = 6.68$ .

71

### 72 Section 4. Probability of stormwater network failure

73 The probability of specific flood volume for the limiting value of  $p_{m,cr}$  (exceeding it indicates that  $\kappa > 13$   
 74  $\text{m}^3 \cdot \text{ha}^{-1}$  can be written as:

$$75 \quad p_{m,cr} = \frac{\exp(X)}{1 + \exp(X)} \quad (7)$$

76 By transforming equation (7), it can be stated that:

$$77 \quad X = \ln\left(\frac{p_{m,cr}}{1 - p_{m,cr}}\right) \quad (8)$$

78 Knowing that  $X$  is a linear combination of the independent variables, the relationship can be written:

$$79 \quad X = X_{rain} + X_{catchm} + \left(\sum_{k=1}^m \alpha_k \cdot x_k + \alpha_{nsew} \cdot n_{sew}\right) \quad (9)$$

80 Comparing sides (8), (9) obtained:

$$81 \quad X_{rain} + X_{catchm} + \left(\sum_{k=1}^m \alpha_k \cdot x_k + \alpha_{nsew} \cdot n_{sew}\right) = \ln\left(\frac{p_{m,cr}}{1 - p_{m,cr}}\right) \quad (10)$$

82 By transforming equation (10), the value of  $n_{sew}$  can be determined from the formula:

$$83 \quad n_{sew} = \frac{1}{\alpha_{nsew}} \cdot \left[ \ln\left(\frac{p_{m,cr}}{1 - p_{m,cr}}\right) - X_{rain} - X_{catch} - \sum_{k=1}^m \alpha_k \cdot x_k \right] \quad (11)$$

84 **Table. S3. Values of coefficients ( $\alpha_i$ ), standard deviations ( $\sigma_i$ ), test probabilities (p) for the logit model to calculate the**  
 85 **probability of specific flood volume.**

86

Variable	Value ( $\alpha_i$ )	St. derivation ( $\sigma_i$ )	p – test
Intercept	-54.146	1.863	< 0.0001
$t_r$	-0.218	0.001	< 0.0001
$P_t$	4.055	0.036	< 0.0001
$\alpha$	0.235	0.012	< 0.0001
$n_{imp}$	-79.397	1.251	< 0.0001
$d_{imp}$	-0.072	0.006	< 0.0001
$\beta$	6.233	0.051	< 0.0001
$\gamma$	0.333	0.043	< 0.0001
$n_{sew}$	234.125	1.145	< 0.0001
Imp	79.403	4.836	< 0.0001
Vk	-0.010	0.000	< 0.0001
Gk	-1967.036	113.936	< 0.0001
Jkp	-20.331	6.775	0.0027
Impd	42.912	2.389	< 0.0001
Gkd	-1169.004	66.862	< 0.0001

87

88

89

90 **Table. S4. Agreement of the results of calculating the probability of exceeding the specific flood volume with the logistic**  
 91 **regression model (LRM) and SWMM**

	Sub - catchment								
$t_r$ [min]	J	K	L	M	N	O	P	R	S
variant I									
30	+	+	+	+	+	+	+	+	+
40	+	+	+	+	+	+	+	+	+
50	+	+	+	+	+	+	+	+	+
60	+	+	+	+	+	+	+	-	-
variant III									
30	+	+	+	+	+	+	+	+	+
40	+	+	+	+	+	+	+	+	+
50	+	+	+	+	+	+	+	+	+
60	+	+	+	+	+	+	-	-	+

92  
 93  
 94  
 95  
 96  
 97  
 98  
 99  
 100  
 101  
 102  
 103  
 104  
 105  
 106  
 107  
 108  
 109  
 110  
 111  
 112

113 **Table S5. Computational scenarios assumed for the verification of the obtained LRM by means of SWMM**

114

Var	±	Impd			Gk			Gkd			Vk			Jkp		
		+20	0	-20	+20	0	-20	+20	0	-20	+20	0	-20	+20	0	-20
Imp	+20	+	+	+	+	+	+	+	+	+	+	+	+	+	+	+
	0	+	+	+	+	+	+	+	+	+	+	+	+	+	+	+
	-20	+	+	+	+	+	+	+	+	+	+	+	+	+	+	+
Impd	+20				+	+	+	+	+	+	+	+	+	+	+	+
	0				+	+	+	+	+	+	+	+	+	+	+	+
	-20				+	+	+	+	+	+	+	+	+	+	+	+
Gk	+20							+	+	+	+	+	+	+	+	+
	0							+	+	+	+	+	+	+	+	+
	-20							+	+	+	+	+	+	+	+	+
Gkd	+20										+	+	+	+	+	+
	0										+	+	+	+	+	+
	-20										+	+	+	+	+	+
Vk	+20													+	+	+
	0													+	+	+
	-20													+	+	+

115

116 **Table S6. Results of simulating the number of events ( $\kappa > 13 \text{ m}^3 \cdot \text{ha}^{-1}$ ) by the LRM for sub - catchment J**

Var	±	Impd			Gk			Gkd			Vk			Jkp		
		+20	0	-20	+20	0	-20	+20	0	-20	+20	0	-20	+20	0	-20
Imp	+20	17	14	14	14	14	16	14	14	15	14	14	14	14	14	14
	0	14	12	7	7	12	14	10	12	14	12	12	14	12	12	12
	-20	7	7	4	5	7	8	5	7	7	6	7	7	7	7	7
Impd	+20				13	14	14	14	14	14	14	14	14	14	14	14
	0				7	12	14	10	12	14	12	12	13	12	12	12
	-20				6	7	12	7	7	10	7	7	8	7	7	7
Gk	+20							7	14	10	7	14	8	7	14	7
	0							10	12	14	12	12	13	12	12	12
	-20							14	7	14	14	7	14	14	7	14
Gkd	+20										9	14	7	10	14	10
	0										12	12	8	12	12	12
	-20										14	7	14	14	7	14
Vk	+20													12	14	12
	0													12	12	12
	-20													13	7	13

117

118 Table S7. Differences in simulation results of the number of events ( $\kappa > 13 \text{ m}^3 \cdot \text{ha}^{-1}$ ) by LRM and SWMM for sub-  
 119 catchment J

Var	±	Impd			Gk			Gkd			Vk			Jkp		
		+20	0	-20	+20	0	-20	+20	0	-20	+20	0	-20	+20	0	-20
Imp	+20	3	3	2	2	3	2	2	3	3	2	3	3	2	3	2
	0	3	2	1	2	2	2	2	2	2	3	2	3	2	2	2
	-20	1	1	0	1	1	1	1	1	0	1	1	1	1	1	1
Impd	+20				2	3	2	2	3	3	2	3	2	2	3	2
	0				2	2	2	2	2	2	3	2	3	2	2	2
	-20				1	1	3	1	1	2	1	1	2	1	1	1
Gk	+20							1	3	2	1	3	2	2	3	1
	0							2	2	2	3	2	3	2	2	2
	-20							3	1	2	3	1	3	2	1	2
Gkd	+20										2	3	2	2	3	2
	0										2	2	3	2	2	2
	-20										2	1	2	2	1	3
Vk	+20													2	3	2
	0													2	2	2
	-20													2	1	2

120

121 Table S8. Results of simulating the number of events ( $\kappa > 13 \text{ m}^3 \cdot \text{ha}^{-1}$ ) by the LRM model for sub-catchment O

Var	±	Impd			Gk			Gkd			Vk			Jkp		
		+20	0	-20	+20	0	-20	+20	0	-20	+20	0	-20	+20	0	-20
Imp	+20	14	14	8	9	14	14	13	14	14	12	14	14	14	14	12
	0	14	7	5	6	7	12	7	7	8	7	7	9	7	7	7
	-20	7	5	3	4	5	7	4	5	5	4	5	6	5	5	4
Impd	+20				8	14	14	12	14	14	11	14	14	13	14	13
	0				6	7	12	7	7	8	7	7	9	7	7	7
	-20				4	5	7	5	5	6	4	5	7	5	5	5
Gk	+20							5	14	7	5	14	7	6	14	6
	0							7	7	8	7	7	9	7	7	7
	-20							11	5	13	8	5	14	12	5	12
Gkd	+20										6	14	8	7	14	7
	0										7	7	9	7	7	7
	-20										7	5	12	8	5	8
Vk	+20													7	14	7
	0													7	7	7
	-20													9	5	10

122 Table S9. Differences in simulation results of the number of events ( $\kappa > 13 \text{ m}^3 \cdot \text{ha}^{-1}$ ) by LRM and SWMM for  
 123 sub – catchment O

Var	±	Impd			Gk			Gkd			Vvk			Jkp		
		+20	0	-20	+20	0	-20	+20	0	-20	+20	0	-20	+20	0	-20
Impd	+20	3	2	1	2	2	3	2	2	2	2	2	3	3	2	2
	0	2	2	1	1	2	3	1	2	2	1	2	2	2	2	1
	-20	1	1	0	0	1	1	1	1	1	1	1	2	0	1	1
Impd	+20				1	2	3	3	2	1	2	2	2	3	2	3
	0				1	2	3	1	2	2	1	2	2	2	2	1
	-20				1	1	0	1	1	1	1	1	1	1	1	1
Gk	+20							1	2	1	1	2	2	1	2	1
	0							1	2	2	1	2	2	2	2	1
	-20							2	1	2	2	1	3	2	1	3
Gkd	+20										1	2	2	1	2	1
	0										1	2	2	2	2	1
	-20										1	1	3	1	1	1
Vvk	+20													1	2	1
	0													2	2	1
	-20													2	1	3

124  
 125 Table S10. Results of simulating the number of events ( $\kappa > 13 \text{ m}^3 \cdot \text{ha}^{-1}$ ) by the LRM for sub-catchment S

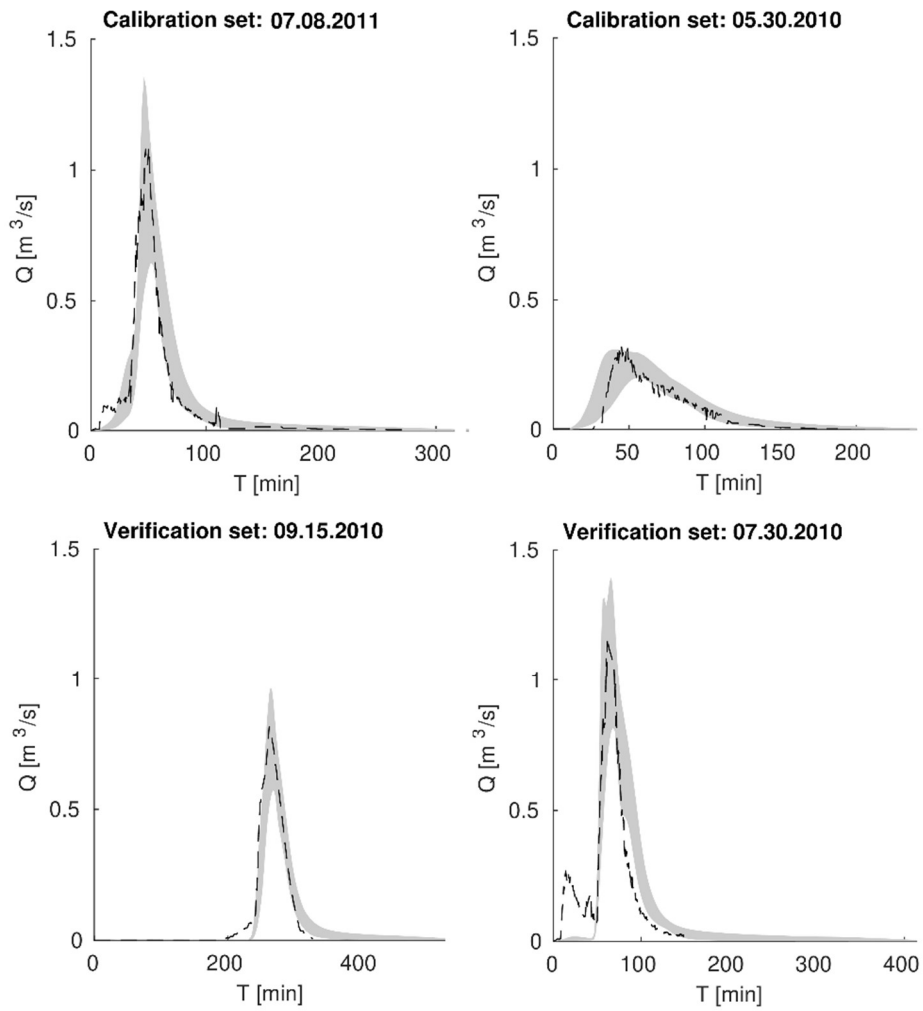
Var	±	Impd			Gk			Gkd			Vvk			Jkp		
		+20	0	-20	+20	0	-20	+20	0	-20	+20	0	-20	+20	0	-20
Impd	+20	22	16	14	14	16	21	14	16	16	14	16	21	16	16	16
	0	15	14	9	11	14	14	14	14	14	12	14	14	14	14	14
	-20	13	7	5	5	7	12	5	7	7	6	7	11	7	7	7
Impd	+20				14	16	21	14	16	15	14	16	19	15	16	15
	0				11	14	14	14	14	14	12	14	14	14	14	14
	-20				7	7	14	8	7	9	7	7	13	9	7	9
Gk	+20							10	16	12	7	16	14	11	16	11
	0							14	14	14	12	14	14	14	14	14
	-20							14	7	14	14	7	16	14	7	14
Gkd	+20											16	14	14	16	14
	0											14	14	14	14	14
	-20											7	14	14	7	14
Vvk	+20														16	12
	0														14	14
	-20														7	14



126 Table S11. Differences in simulation results of the number of events ( $\kappa > 13 \text{ m}^3 \cdot \text{ha}^{-1}$ ) by LRM and SWMM for  
 127 sub – catchment J

Var	±	Impd			Gk			Gkd			Vk			Jkp		
		+20	0	-20	+20	0	-20	+20	0	-20	+20	0	-20	+20	0	-20
Imp	+20	4	3	3	2	3	2	3	3	2	3	3	4	3	3	2
	0	3	3	2	2	2	2	2	2	2	2	2	2	3	2	2
	-20	3	1	1	1	1	2	1	1	1	0	1	2	1	1	1
Impd	+20				2	3	4	3	3	2	2	3	3	3	3	2
	0				2	2	2	2	2	2	2	2	2	3	2	2
	-20				2	1	3	1	1	1	0	1	3	2	1	1
Gk	+20							2	3	2	1	3	3	2	3	2
	0							2	2	2	2	2	2	3	2	2
	-20							2	1	3	2	1	3	2	1	2
Gkd	+20											3	3	2	3	2
	0											2	2	3	2	2
	-20											1	3	2	1	2
Vk	+20														3	2
	0														2	2
	-20														1	2

128  
 129  
 130  
 131  
 132  
 133  
 134  
 135  
 136  
 137  
 138  
 139  
 140  
 141  
 142  
 143  
 144  
 145



146

147 **Figure S1. Comparison of the measured hydrographs of stormwater runoff from the catchment with 95% confidence**

148

**intervals determined via the SWMM model.**

149

150

151

152

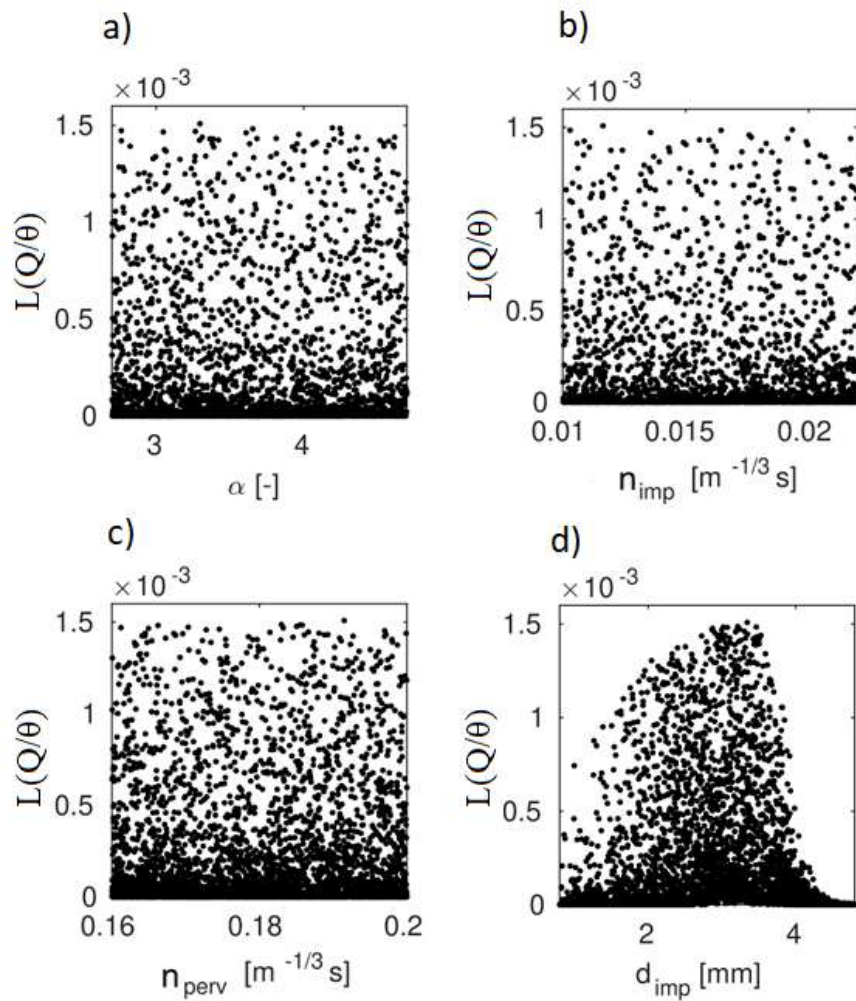
153

154

155

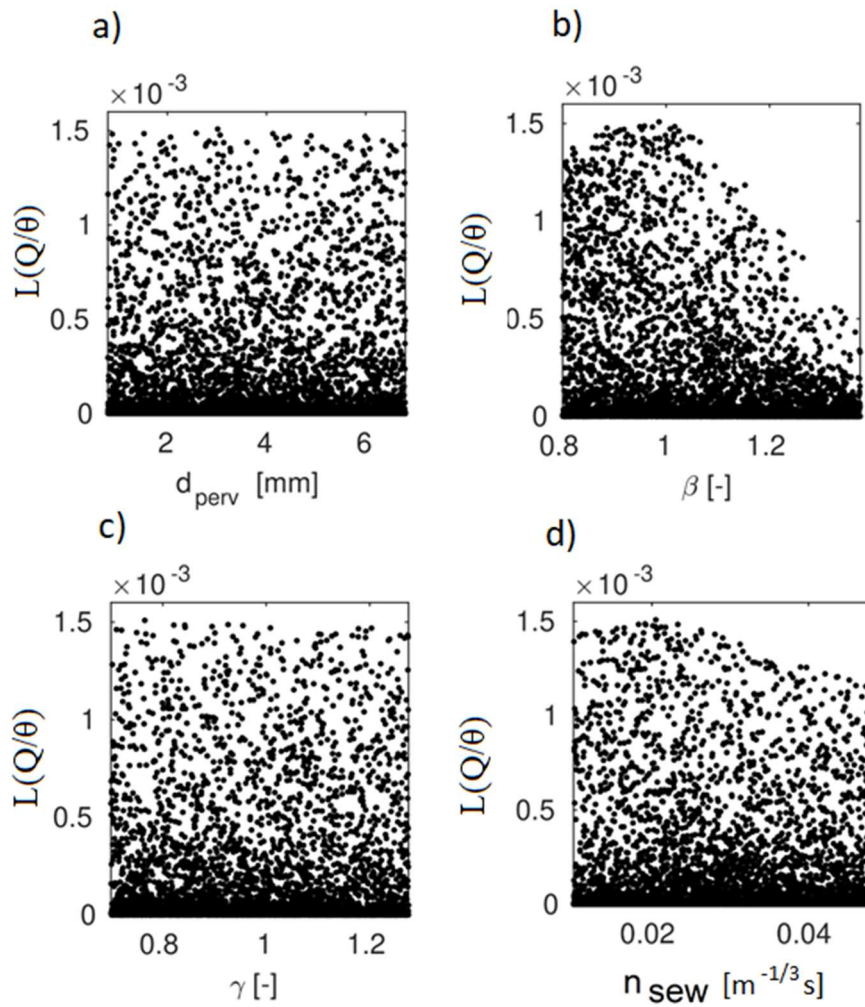
156

157



159

160 **Figure S2. Influence of (a) coefficient for flow path width ( $\alpha$ ), (b) Manning roughness coefficient for impervious areas**  
 161 **( $n_{imp}$ ), (c) Manning roughness coefficient for pervious areas ( $n_{per}$ ) and retention depth of impervious areas ( $d_{imp}$ ) on**  
 162 **the likelihood function ( $L(Q/\theta)$ ).**



163

164

165

166

167

168

169

170

171

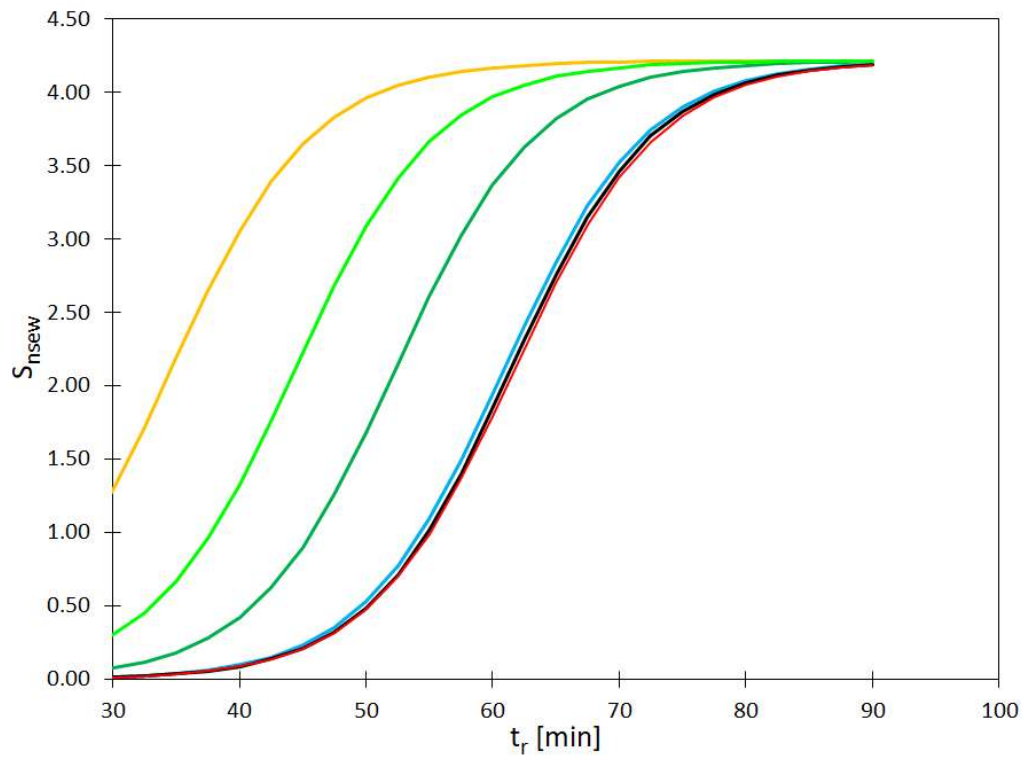
172

173

174

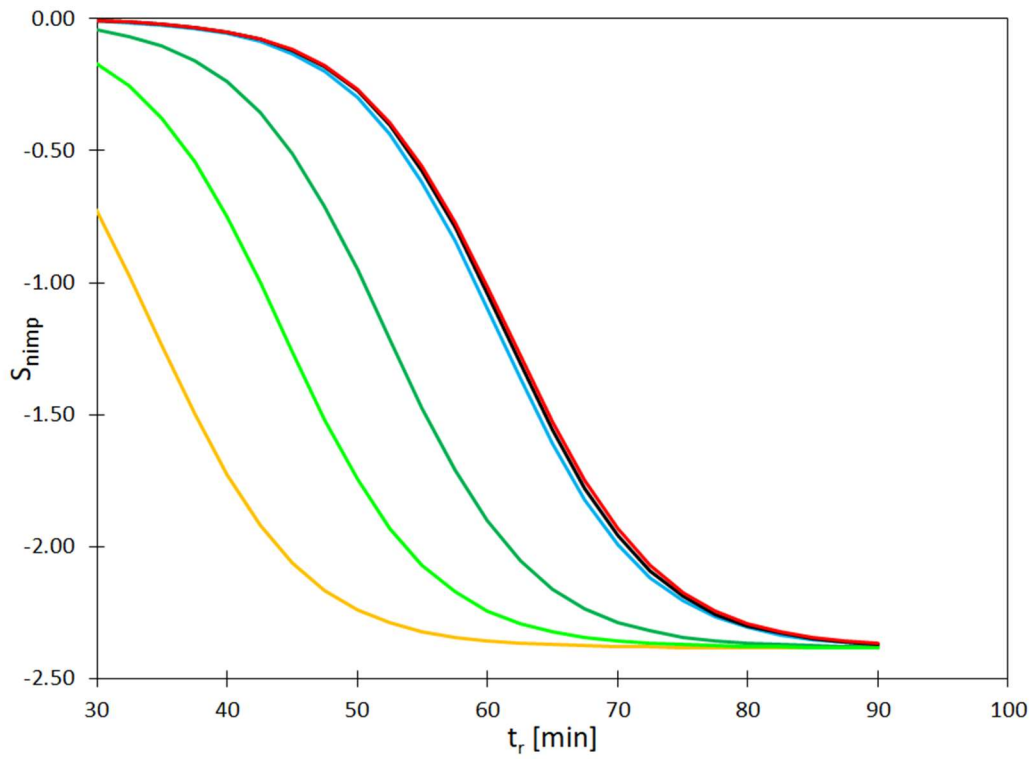
175

**Figure S3. Influence of (a) retention depth of pervious areas ( $d_{\text{perv}}$ ), (b) correction coefficient for percentage of impervious areas ( $\beta$ ), (c) correction coefficient for sub-catchments slope ( $\gamma$ ) and Manning roughness coefficient for sewer channels ( $n_{\text{sew}}$ ) on the likelihood function ( $L(Q/\theta)$ ).**



176

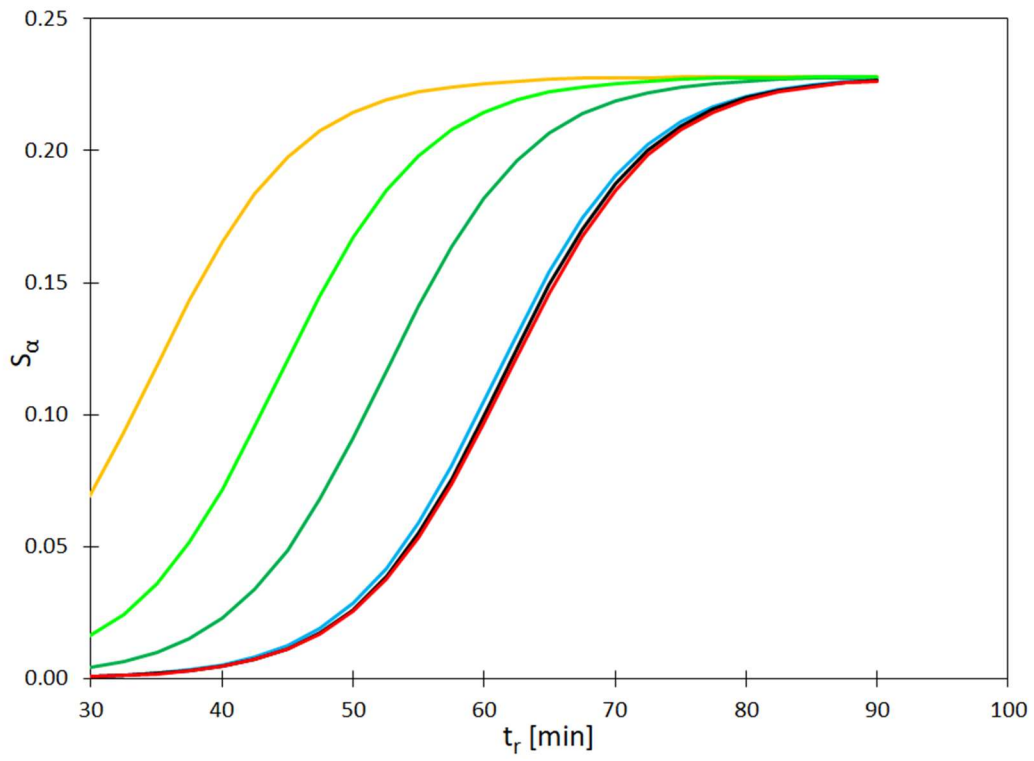
177 **Figure S4. Influence of rainfall duration ( $t_r$ ) depending on catchment and stormwater network characteristics (Imp,**  
 178 **Impd, Vk, Jkp, Gk) on the sensitivity coefficient  $S_{nsew}$ .**  
 179



180

181 **Figure S5. Influence of rainfall duration ( $t_r$ ) depending on catchment and stormwater network characteristics (Imp,**  
 182 **Impd, Vk, Jkp, Gk) on the sensitivity coefficient  $S_{nimp}$ .**

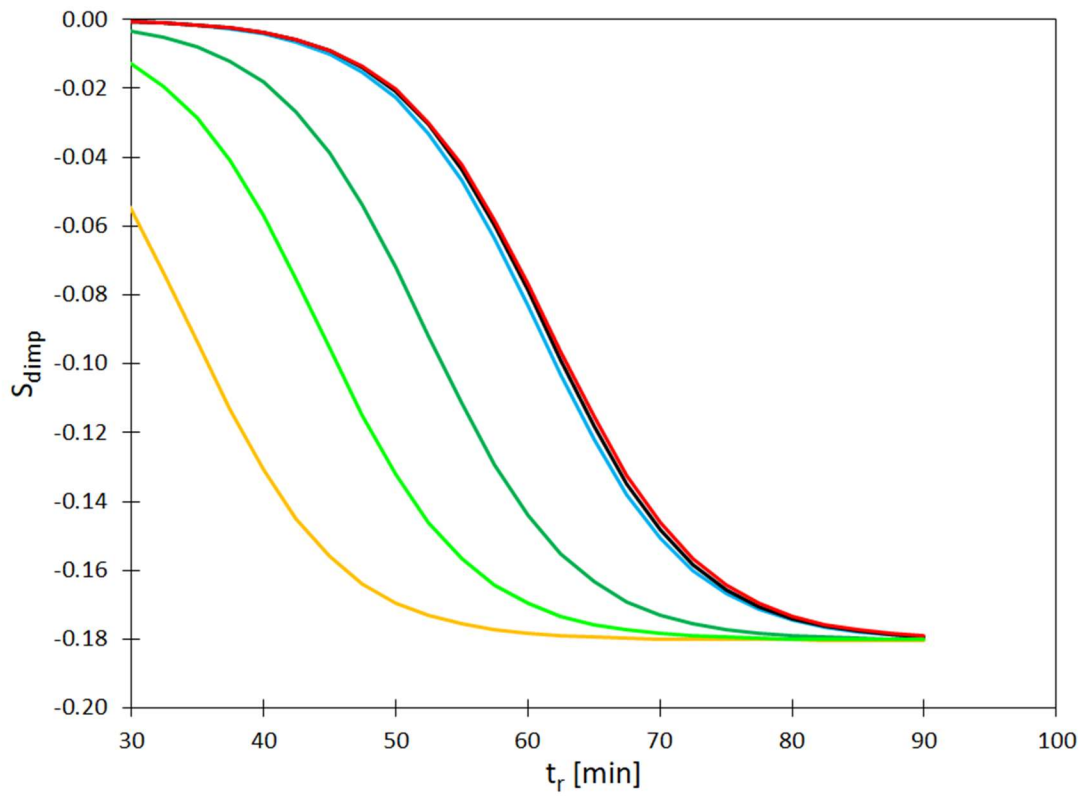
183



184

185 **Figure S6. Influence of rainfall duration ( $t_r$ ) depending on catchment and stormwater network characteristics (Imp,**  
 186 **Impd, Vk, Jkp, Gk) on the sensitivity coefficient  $S_\alpha$ .**

187



188

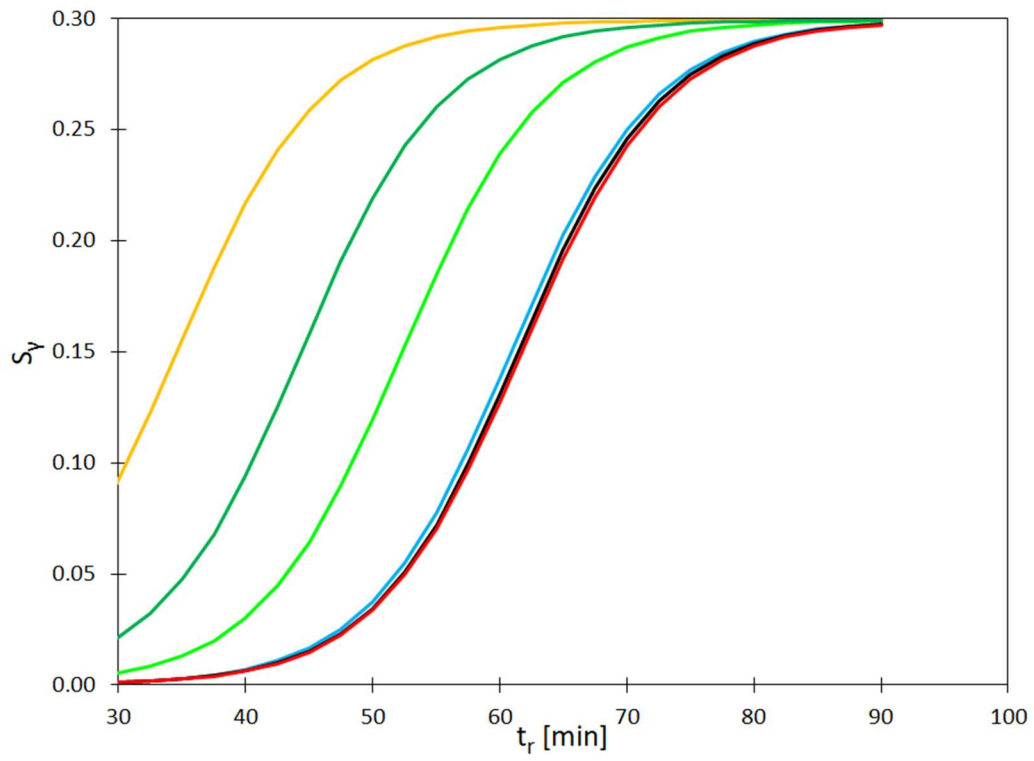
189

190

191

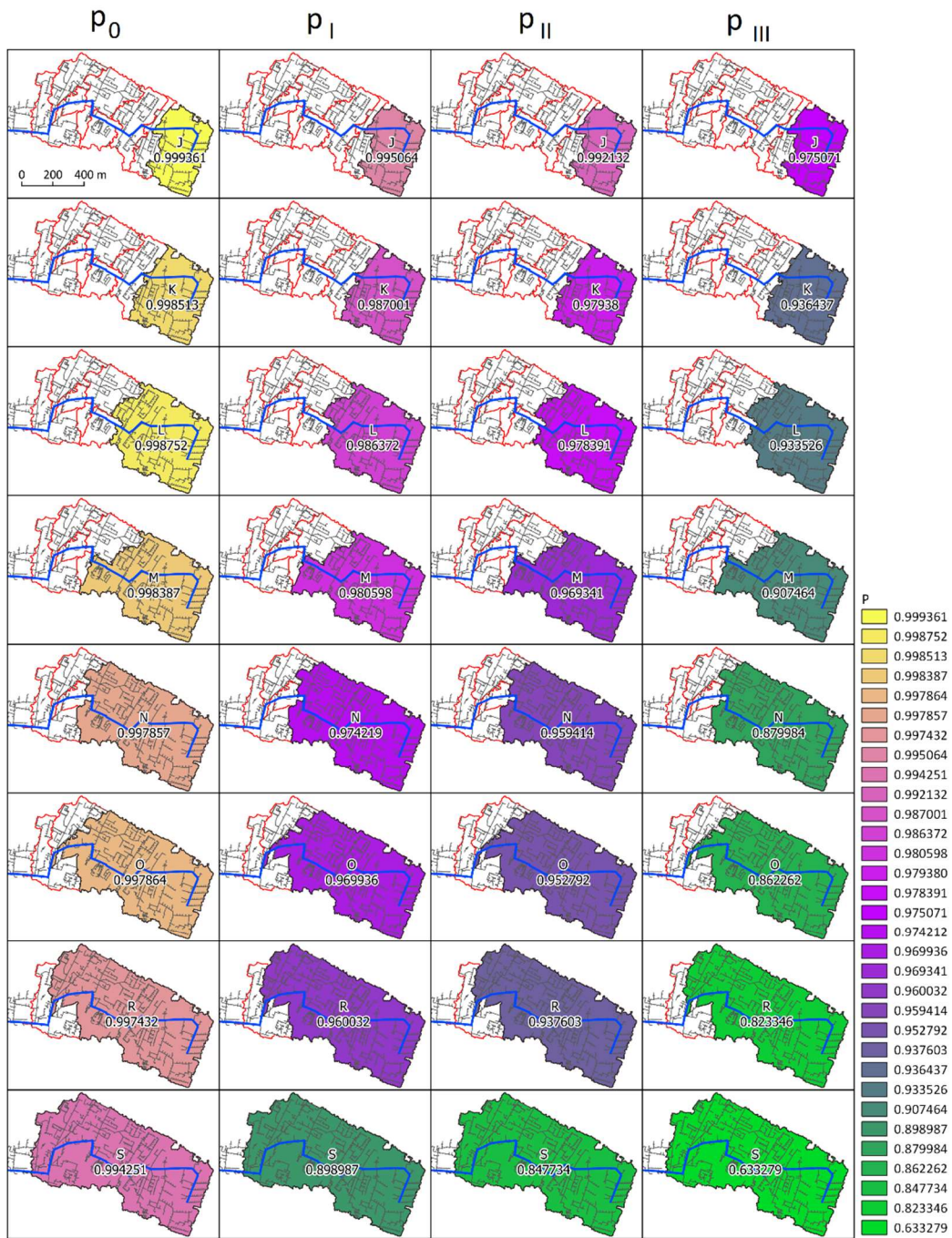
**Figure S7. Influence of rainfall duration ( $t_r$ ) depending on catchment and stormwater network characteristics (Imp, Impd, Vk, Jkp, Gk) on the sensitivity coefficient  $S_{dimp}$ .**





192  
 193  
 194  
 195

**Figure S8. Influence of rainfall duration ( $t_r$ ) depending on catchment and stormwater network characteristics (Imp, Impd, Vk, Jkp, Gk) on the sensitivity coefficient  $S_\gamma$ .**



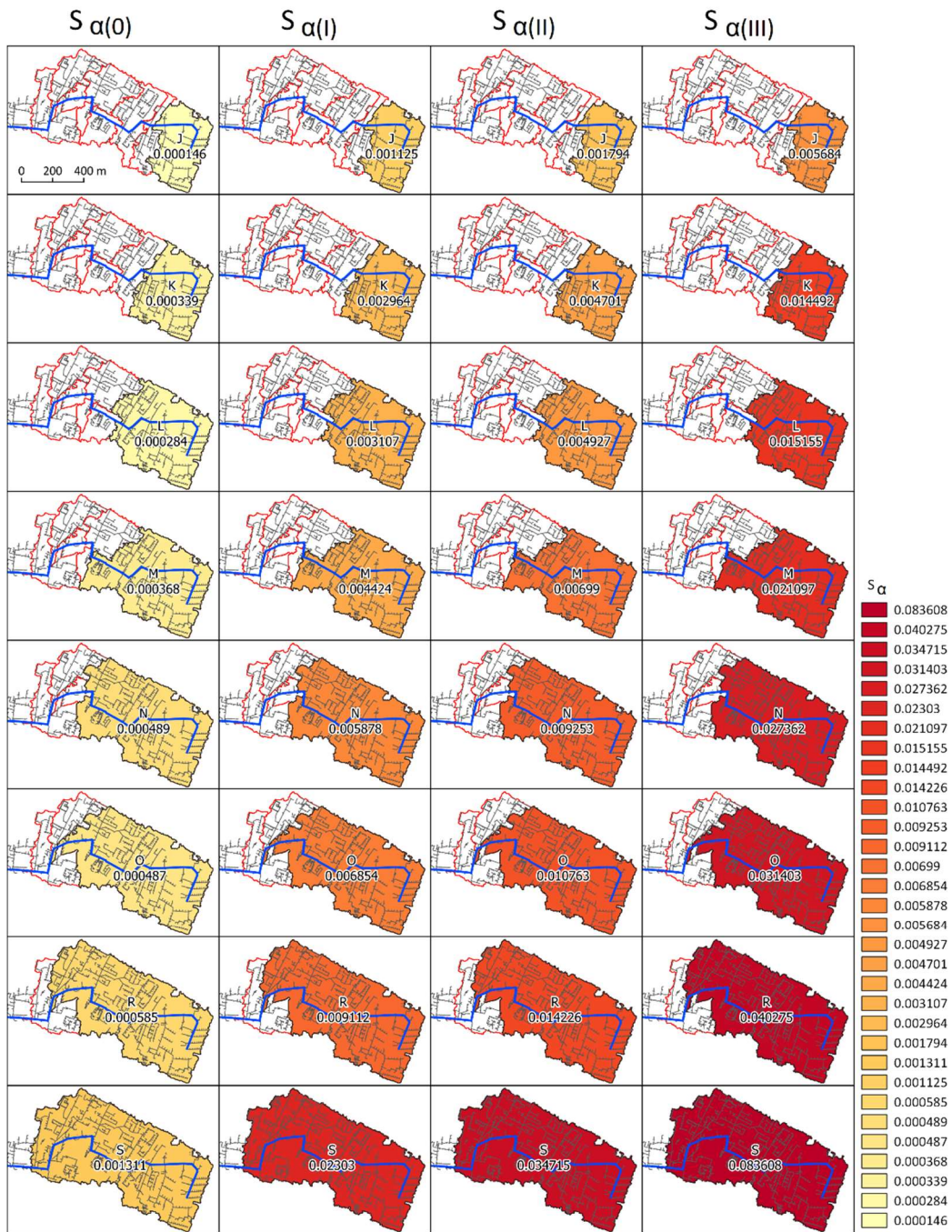
196

197

198

199

**Figure S9. Probability of specific flood volume for separate sub-catchments (J, K, L, M, N, O, R, S) for the current state and corrective variants (I, II, III).**

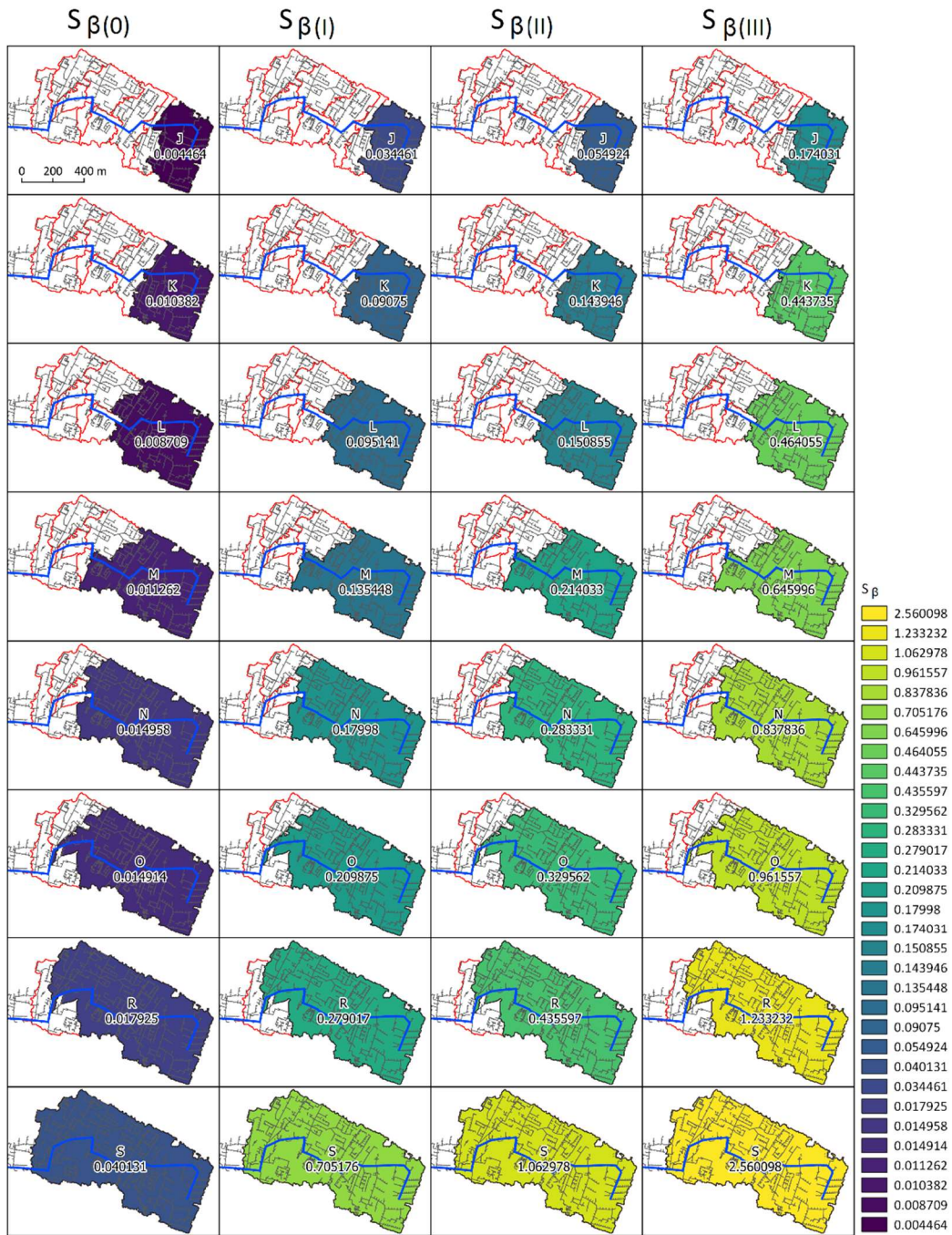


200

201 **Figure S10. Sensitivity coefficient  $S_{\alpha}$  for separated of the sub-catchments (J, K, L, M, N, O, R, S) for the current state**  
 202 **and corrective variants (I, II, III).**

203

204

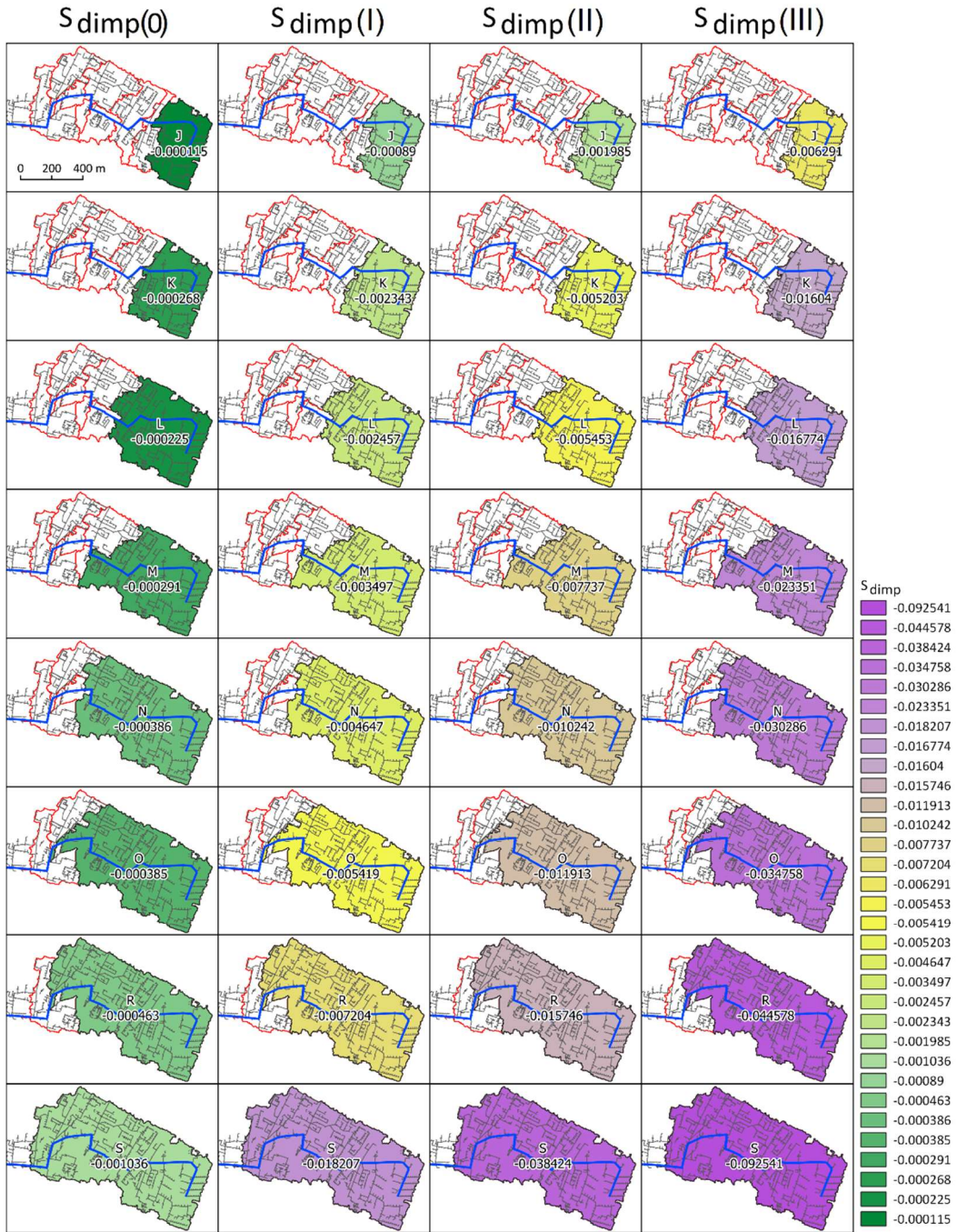


205

206 **Figure S11. Sensitivity coefficient  $S_{\beta}$  for separated of the sub-catchments (J, K, L, M, N, O, R, S) for the current state**  
 207 **and corrective variants (I, II, III).**

208

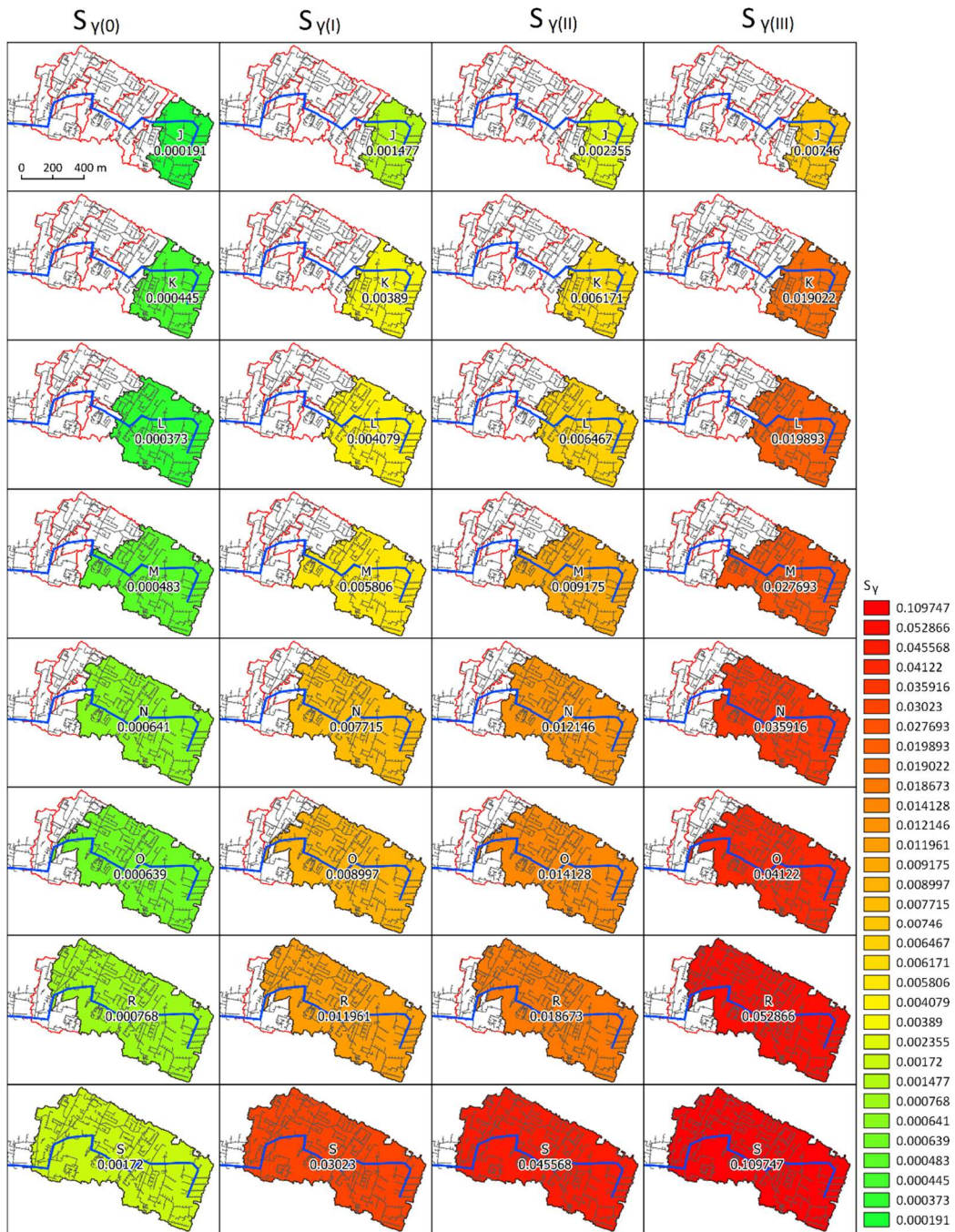
209



211

212 **Figure S12. Sensitivity coefficient  $S_{dimp}$  for separated of the sub-catchments (J, K, L, M, N, O, R, S) for the current**  
 213 **state and corrective variants (I, II, III).**

214

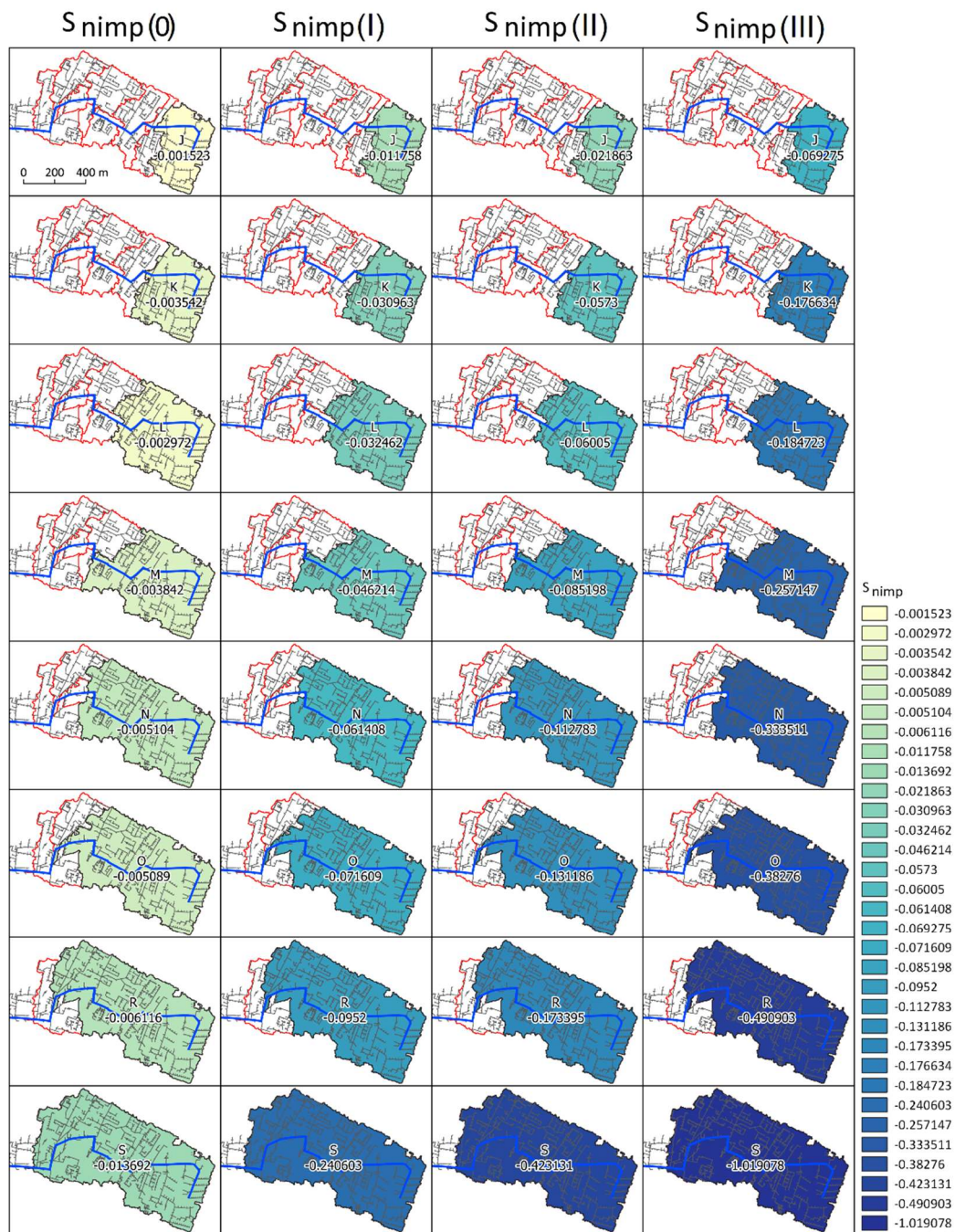


215

216

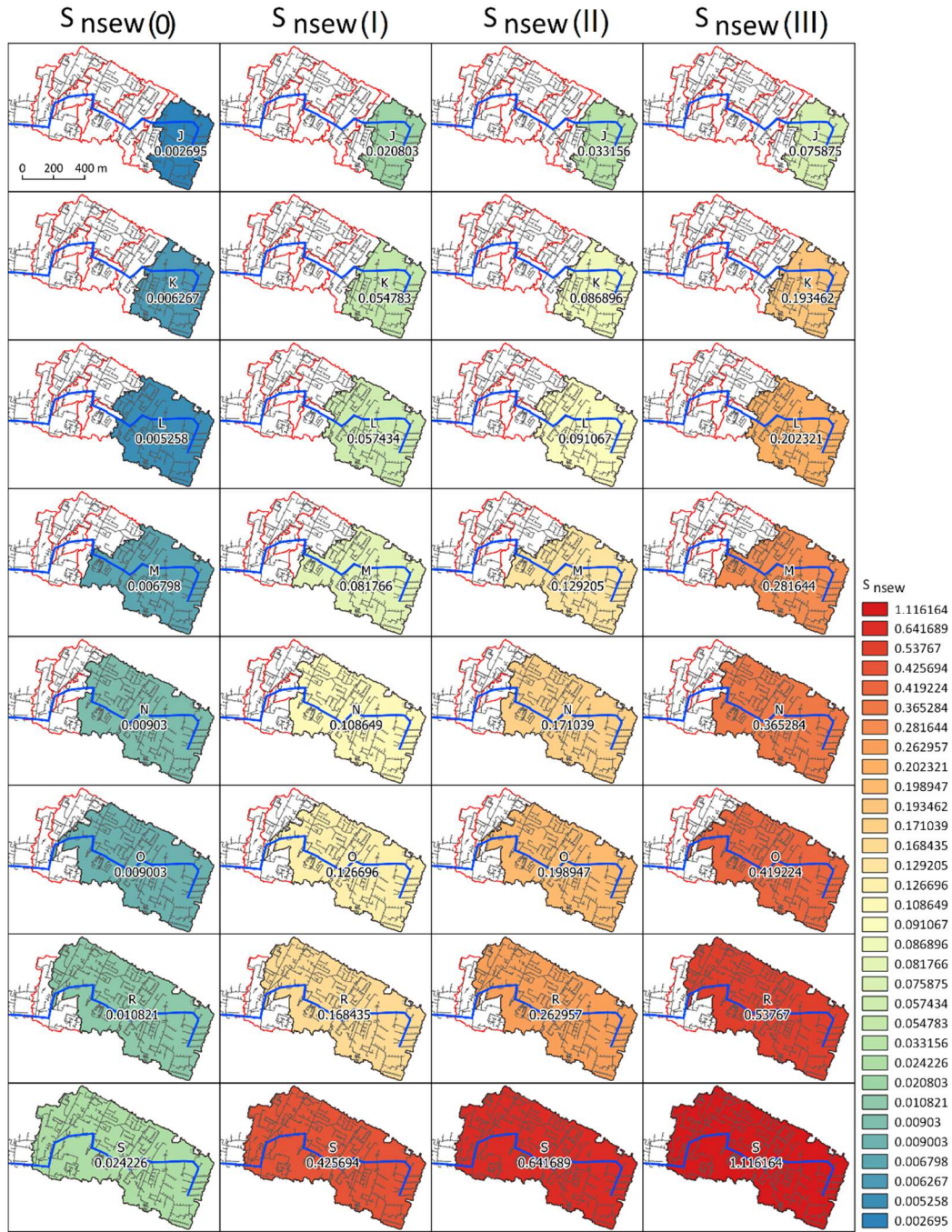
217 **Figure S13. Sensitivity coefficient  $S_Y$  for separated of the sub-catchments (J, K, L, M, N, O, R, S) for the current state**  
 218 **and corrective variants (I, II, III).**

219



221  
222

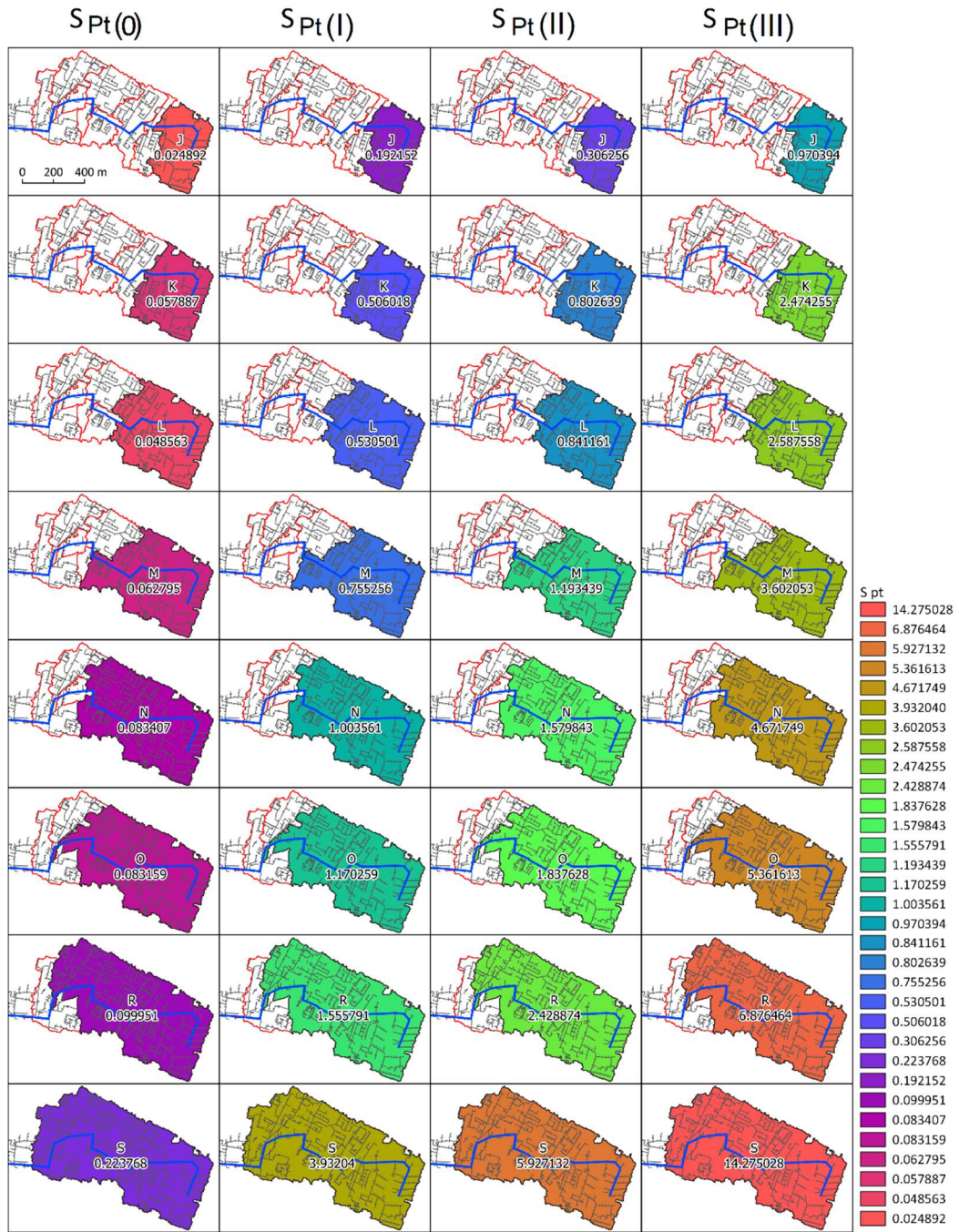
223 **Figure S14. Sensitivity coefficient  $S_{nimp}$  for separated of the sub-catchments (J, K, L, M, N, O, R, S) for the current**  
224 **state and corrective variants (I, II, III).**



226

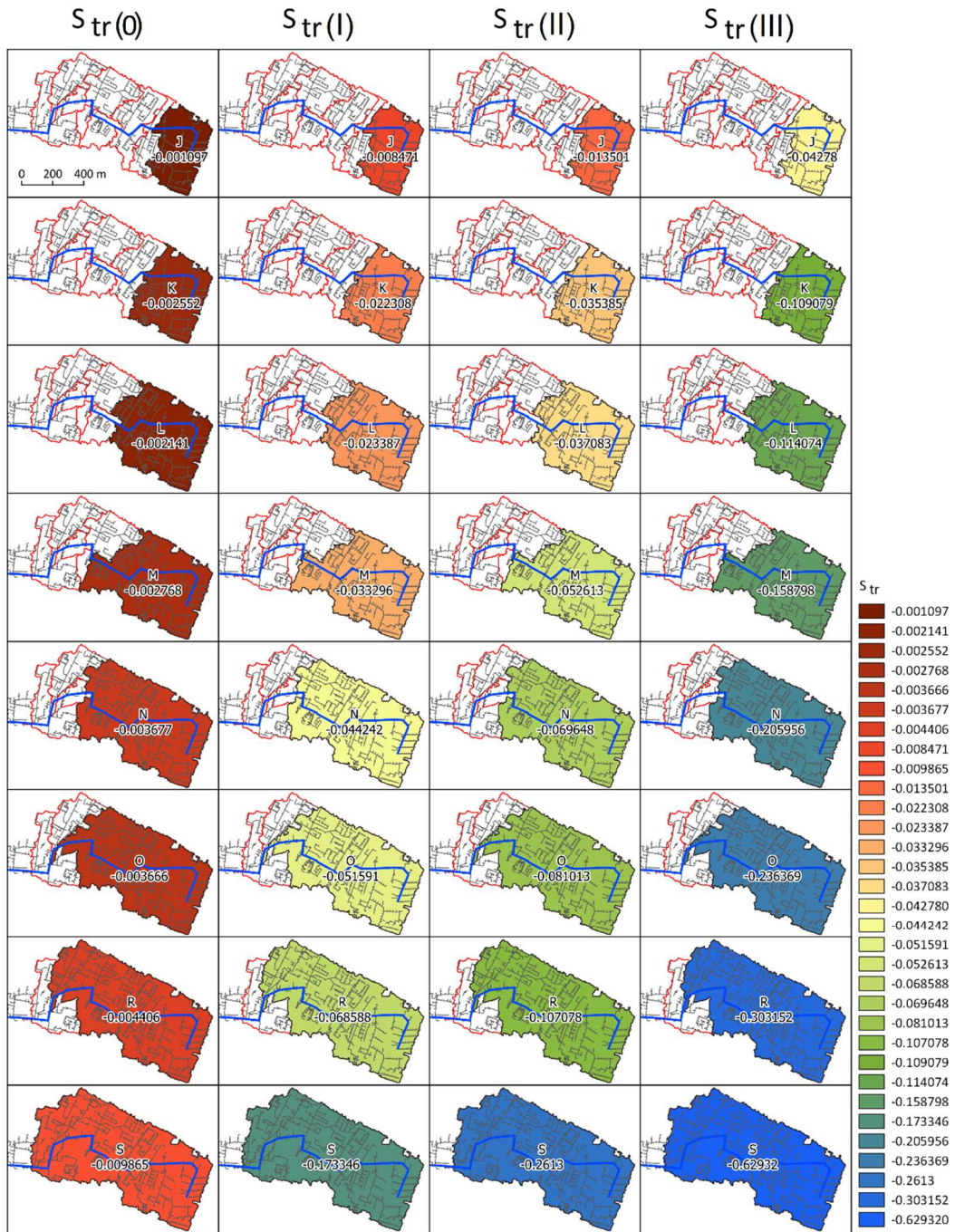
227 **Figure S15. Sensitivity coefficient  $S_{nsew}$  for separated of the sub-catchments (J, K, L, M, N, O, R, S) for the current**  
 228 **state and corrective variants (I, II, III).**





232 Figure S16. Sensitivity coefficient  $S_{Pt}$  for separated of the sub-catchments (J, K, L, M, N, O, R, S) for the current state

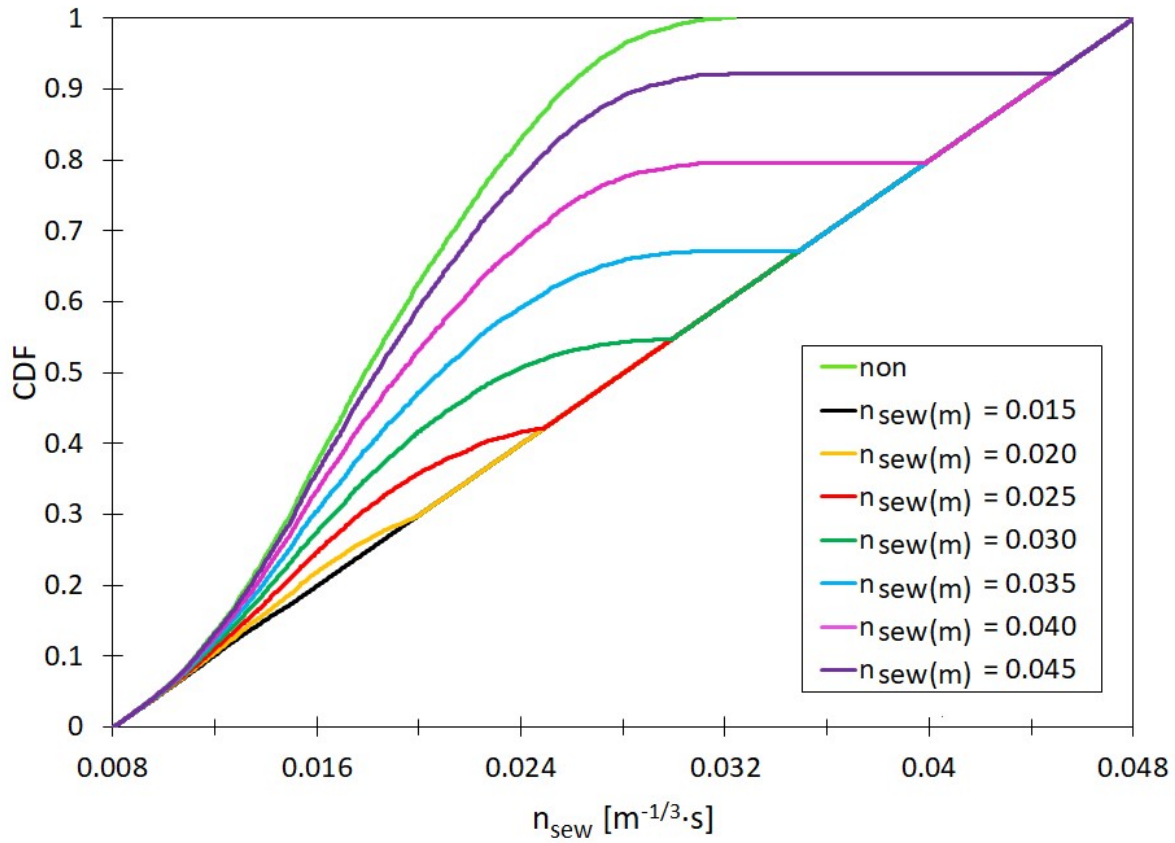
and corrective variants (I, II, III).



235

236 **Figure S17. Sensitivity coefficient  $S_{tr}$  for separated of the sub-catchments (J, K, L, M, N, O, R, S) for the current state**  
 237 **and corrective variants (I, II, III).**

238



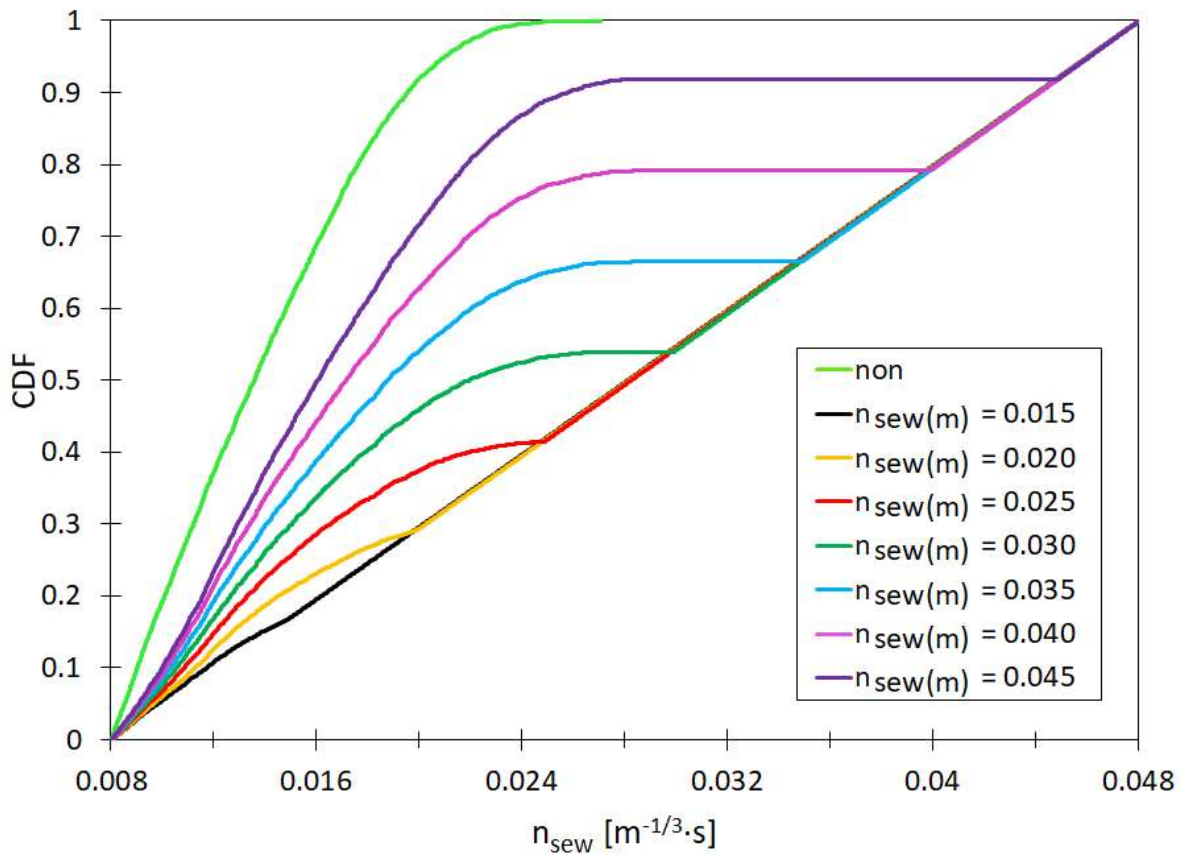
241

242

**Figure S18. Empirical distributions of Manning roughness coefficients of channels ( $n_{sew}$ ) for  $n_{sew(m)}=0.015 - 0.045 \text{ m}^{-1/3} \cdot \text{s}$ ,  $Imp = 0.35$  and  $Impd = 0.42$ .**

243

244



245  
 246  
 247  
 248  
 249  
 250

**Figure S19. Empirical distributions of Manning roughness coefficients for channels ( $n_{sew}$ ) for  $n_{sew(m)}=0.015 - 0.045 m^{-1/3} \cdot s$ ,  $Imp = 0.35$  and  $Impd = 0.40$ .**